Efficient RNase H–Directed Cleavage of RNA Promoted by Antisense DNA or 2'F–ANA Constructs Containing Acyclic Nucleotide Inserts

ARTICLE *in* JOURNAL OF THE AMERICAN CHEMICAL SOCIETY · FEBRUARY 2003

Impact Factor: 12.11 · DOI: 10.1021/ja025557o · Source: PubMed

7 AUTHORS, INCLUDING:

Ekaterina Viazovkina
McGill University
17 PUBLICATIONS **185** CITATIONS
SEE PROFILE

Mohamed Ibrahim Elzagheid
Jubail Industrial College
25 PUBLICATIONS **149** CITATIONS
SEE PROFILE

Michael Parniak
University of Pittsburgh
184 PUBLICATIONS **5,953** CITATIONS
SEE PROFILE

J|A|C|S
ARTICLES
Published on Web 12/20/2002

Efficient RNase H-Directed Cleavage of RNA Promoted by Antisense DNA or 2′F-ANA Constructs Containing Acyclic Nucleotide Inserts

Maria M. Mangos, Kyung-Lyum Min, Ekaterina Viazovkina, Annie Galarneau, Mohamed I. Elzagheid, Michael A. Parniak,† and Masad J. Damha*

Contribution from McGill University, Departments of Chemistry and Experimental Medicine, Montreal, QC, Canada

Received January 10, 2002; E-mail: masad.damha@mcgill.ca

Abstract: The ability of modified antisense oligonucleotides (AONs) containing acyclic interresidue units to support RNase H-promoted cleavage of complementary RNA is described. Manipulation of the backbone and sugar geometries in these conformationally labile monomers shows great benefits in the enzymatic recognition of the nucleic acid hybrids, while highlighting the importance of local strand conformation on the hydrolytic efficiency of the enzyme more conclusively. Our results demonstrate that the duplexes support remarkably high levels of enzymatic degradation when treated with human RNase HII, making them efficient mimics of the native substrates. Furthermore, interesting linker-dependent modulation of enzymatic activity is observed during in vitro assays, suggesting a potential role for this AON class in an RNase H-dependent pathway of controlling RNA expression. Additionally, the butyl-modified 2′F-ANA AONs described in this work constitute the first examples of a nucleic acid species capable of eliciting high RNase H activity while possessing a highly flexible molecular architecture at predetermined sites along the AON.

Introduction

Antisense oligonucleotides (AONs) represent an attractive and promising class of clinically useful compounds that are rationally designed to alter gene expression patterns.[1] As more sophisticated methods evolve for their construction, their widespread use in functional genomics, drug target validation, and as human therapeutics may soon be realized.[2] Good exo- and endonucleolytic robustness, efficient cell entry, and tight and specific binding with their intended genetic targets in the presence of cellular proteins[2c] are few of the criteria important for the chemotherapeutic potential of AONs.

Additionally, a desirable mechanism which could provide a catalytic mode of supressing gene activity in eukaryotic cells relies upon the activity of ribonuclease H (RNase H), a ubiquitous enzyme of many vital intracellular functions.[3] These activities ultimately culminate in the destruction of the RNA component when duplexed with DNA or a suitable AON variant of the latter.[4] Thus, a single enzyme-active AON can ideally induce the specific destruction of multiple copies of an RNA transcript (i.e., AON recycling) and exhibit greater biological activity than those that do not activate RNase H.[1a] To date, however, most AONs are deficient in one or more of these requisite traits.

Indeed, oligonucleotide "gapmer" modifications that combine intervening enzyme-active AON segments (e.g., DNA) with conformationally restricted residues (e.g., 2′-*O*-alkyl RNA) at the periphery may still effect cleavage of their intended targets.[5] However, these usually focus on preorganizing the antisense strand to adopt a more compatible structure that affords tighter target binding, while compromising high RNase H induction.[6]

Our previous discovery[7] that arabinose-derived AON (e.g., ANA, 2′F-ANA) can elicit RNase H degradation of target RNA has established that an O4′-*endo* conformation[8] in the antisense sugar residues is of prime importance;[8a,9] yet, other carbohydrate-modified AONs with this same antipodal bias have been unable

* To whom correspondence should be addressed. Otto Maass Chemistry Bldg., McGill University, 801 Sherbrooke St. W., Montreal, QC, Canada H3A 2K6.

† Current address: Department of Medicine, University of Pittsburgh, Scaife Hall, 3550 Terrace St., Pittsburgh, PA 15261.

(1) (a) Uhlmann, E.; Peyman, A. *Chem. Rev.* **1990**, *90*, 543−584. (b) Crooke, S. T.; Bennett, C. F. *Annu. Rev. Pharmacol. Toxicol.* **1996**, *36*, 107−129.
(2) (a) Eckstein, F. *Annu. Rev. Biochem.* **1985**, *54*, 367−402. (b) Akhtar, S.; Agrawal, S. *Trends Pharmacol. Sci.* **1997**, *18*, 12−18. (c) See, for example: Lebedeva, I.; Stein, C. *Annu. Rev. Pharmacol. Toxicol.* **2001**, *41*, 403−419 and references therein.
(3) (a) Walder, R. Y.; Walder, J. A. *Proc. Natl. Acad. Sci. U.S.A.* **1978**, *75*, 5011−5015. (b) Itaya, M.; Kondo, K. *Nucleic Acids Res.* **1991**, *19*, 4443−4449. (c) Monia, B. P.; Lesnik, E. A.; Gonzalez, C.; Lima, W. F.; McGee, D.; Guinosso, C. J.; Kawasaki, A. M.; Cook, P. D.; Freier, S. M. *J. Biol. Chem.* **1993**, *268*, 14514−14522.
(4) (a) Nakamura, H.; Oda, Y.; Iwai, S.; Inoue, H.; Ohtsuka, E.; Kanaya, S.; Kimura, S.; Katsuda, C.; Katayanagi, K.; Morikawa, K.; Miyashiro, H.; Ikehara, M. *Proc. Natl. Acad. Sci. U.S.A.* **1991**, *88*, 11535−11539. (b) Oda, Y.; Iwai, S.; Ohtsuka, E.; Ishikawa, M.; Ikehara, M.; Nakamura, H. *Nucleic Acids Res.* **1993**, *21*, 4690−4695. (c) Uchiyama, Y.; Miura, Y.; Inoue, H.; Ohtsuka, E.; Ueno, Y.; Ikehara, M. *J. Mol. Biol.* **1994**, *4*, 782−791.
(5) (a) Baker, B. F.; Lot, S. S.; Condon, T. P.; Cheng-Flournoy, S.; Lesnik, E. A.; Sasmor, H. M.; Bennett, C. F. *J. Biol. Chem.* **1997**, *272*, 11994−12000. (b) Freier, S. M.; Altmann, K.-H. *Nucleic Acids Res.* **1997**, *25*, 4429−4443. (c) Nishizaki, T.; Iwai, S.; Ohtsuka, E.; Nakamura, H. *Biochemistry* **1997**, *36*, 2577−2585.
(6) (a) Shen, L. X.; Kandimalla, E. R.; Agrawal, S. *Bioorg. Med. Chem.* **1998**, *6*, 1695−1705. (b) Christensen, N. K.; Peterssen, M.; Nielsen, P.; Jacobsen, J. P.; Olsen, C. E.; Wengel, J. *J. Am. Chem. Soc.* **1998**, *120*, 5458−5463. (c) Nielsen, K. E.; Singh, S. K.; Wengel, J.; Jacobsen, J. P. *Bioconjugate Chem.* **2000**, *11*, 228−238.

10.1021/ja025557o CCC: $25.00

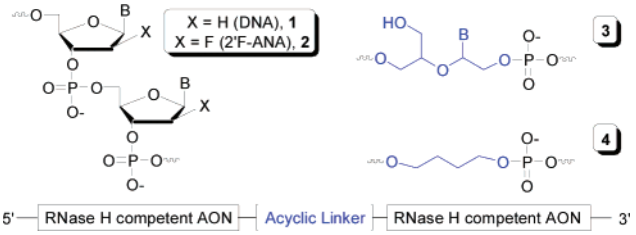

Figure 1. AON constructs containing acyclic internucleotide units.

to sustain the same activity (e.g., [3.3.0]bc-ANA).[6b,10] Thus, we hypothesize that the inherent flexibility of these sugar conformations impacts on the ability of the enzyme[7e,9a] to bind to and recognize hybrids of ANA-derived AON and RNA.

We wished to explore the significance of imparting conformational variability in 2′F-ANA (2′-deoxy-2′-fluoro-β-D-arabinonucleic acid, **2**) to determine whether the insertion of an acyclic residue in a known RNase H-active AON could accelerate the enzymatic degradation. This was accomplished by the systematic introduction of acyclic nucleotides consisting of a 2′,3′-secouridine synthon **3** or a butanediol linker **4** (Figure 1). We surmised that this relatively unconstrained molecular architecture would improve RNase H induction properties as well as provide some insight toward elucidating the structural factors that provide the "optimal" AON/RNA substrate.

Materials and Methods

Synthesis of Acyclic Monomers and AONs. The synthesis of 2′F-ANA monomers of **2** and of mixed backbone AON comprising 2′F-ANA and DNA has already been extensively described elsewhere.[7a,b,f,g] Secouridine 2′-phosphoramidites of **3** were prepared by variations of published protocols.[11] Briefly, the acyclic nucleoside residues consist of a 1-[1,5-dihydroxy-4(*S*)-hydroxymethyl-3-oxapent-2(*R*)-yl]-uracil unit which has been appropriately protected (Scheme 1) and functionalized for oligonucleotide incorporation as described below.

(A) 5′-*O*-MMT-2′,3′-seco-β-D-uridine (3a). To a 0.1 M solution of 5′-monomethoxytrityluridine[12] (5′-MMT-rU, 5.16 g, 10 mmol) in dioxane was added a saturated solution of $NaIO_4$ in H_2O (2.26 g, 10.6 mmol, 1.06 equiv) and the reaction allowed to proceed at room temperature for 2−3 h until complete conversion to the dialdehyde was observed by TLC visualization (R_f 0.52 in CH_2Cl_2:MeOH, 9:1). The reaction was diluted with dioxane (100 mL), filtered to remove $NaIO_3$ salts and followed by in situ reduction of the dialdehyde via treatment with $NaBH_4$ (0.378 g, 10 mmol, 1.0 equiv) for 10−20 min at room temperature. The reaction mixture was quenched with acetone, neutralized with 20% acetic acid, and concentrated to an oil under reduced pressure. The residue was then diluted with CH_2Cl_2 (200 mL) and washed with H_2O. The aqueous layer was back-extracted, and the combined organic layers were dried using anhydrous Na_2SO_4, filtered, and evaporated to give the product as a pure white foam in 98% isolated yield (5.08 g; 9.8 mmol). R_f (CH_2Cl_2:MeOH, 9:1) 0.18; FAB-MS (NBA) 519.6; Calcd 518.57.

(B) 5′-*O*-MMT-2′-*O*-*tert*-butyldimethysilyl-2′,3′-secouridine (3b) and 5′-*O*-MMT-3′-*O*-*tert*-butyldimethysilyl-2′,3′-secouridine (3c). Monoprotection of either of the free hydroxyl functions of **3a** was achieved nonselectively by adding *tert*-butyldimethylsilyl chloride (0.81 g, 5.4 mmol, 1.1 equiv) to a stirred 0.1 M solution of **3a** (2.55 g, 4.9 mmol) in dry THF at 0 °C containing a suspension of $AgNO_3$ (0.92 g, 5.39 mmol, 1.1 equiv). The reaction temperature was returned to room temperature after 20 min and maintained as such for 24 h. The workup was initiated by filtering the mixture directly into an aqueous solution of 5% $NaHCO_3$ (50 mL), followed by extraction of the aqueous layer twice with CH_2Cl_2. The combined organic layers were dried (anhydrous Na_2SO_4), filtered, and evaporated under reduced pressure to give the crude product as a yellow oil. The residue was purified by flash silica gel column chromatography using a gradient of 0−25% acetone in CH_2Cl_2 to recover both monosilyl isomers as pure white foams. Isolated yields for **3b** and **3c** were 22% and 14%, respectively. R_f (CH_2Cl_2:Et_2O, 3:1) **3b**, 0.18; **3c**, 0.05. FAB-MS (NBA) 633.4; Calcd 632.83.

The regioisomers are distinguished on the basis of COSY NMR cross-peak correlations that are used to demonstrate the connectivity of the protons in the acyclosugar. In both spectra, the H1′ protons are split by the nonequivalent H2′ and H2″ protons into a doublet of doublets which suggests a certain degree of structural rigidity around the C1′−C2′ bond. More significantly, a single well-resolved hydroxyl peak is observed for both **3b** and **3c** in DMSO-d_6 which negates rapid chemical exchange of these moieties. As a result, the effect of the protons at C2′ of **3c** is transmitted to the 2′-hydroxyl proton which in turn appears as an overlapping doublet of doublets. In **3b**, splitting of the hydroxyl resonance is also observed; however, it shows correlations with H3′ and H3″ and therefore rules out the presence of a silyl group at the 3′-position. Taken together, these data confirm the assignment of **3b** and **3c** as the 2′- and 3′-monosilylated isomers, respectively.

(C) 5′-*O*-MMT-3′-*O*-*tert*-butyldimethysilyl-2′,3′-secouridine-2′-*O*-[*N*,*N*-diisopropylamino-(2-cyanoethyl)]phosphoramidite (3d). To a nitrogen-purged solution of 4-(dimethylamino)pyridine (DMAP; 12 mg, 0.10 mmol, 0.1 equiv), *N*,*N*-diisopropylethylamine (DIPEA; 0.68 mL, 3.9 mmol, 4 equiv) and **3c** (620 mg, 0.98 mmol) in THF (0.2 M) at 0 °C was added *N*,*N*-diisopropylamino-β-cyanoethylphosphonamidic chloride (0.24 mL, 1.1 mmol, 1.1 equiv) dropwise over 5 min. The immediate appearance of a white precipitate due to the rapid formation of diisopropylethylammonium hydrochloride signified sufficiently anhydrous conditions, and the reaction was allowed to warm to room temperature, whereupon it was stirred for 2.5 h prior to the reaction workup. Briefly, the reaction mixture was diluted with EtOAc (50 mL, prewashed with 5% $NaHCO_3$) and washed with saturated brine (2 × 20 mL). The recovered organic layer was dried (anhydrous Na_2SO_4) and filtered, and the solvent was removed via reduced pressure, yielding a crude yellow oil. Co-evaporation of the crude product with Et_2O afforded a pale yellow foam. Purification of the product by flash silica gel column chromatography using a CH_2Cl_2:hexanes:TEA gradient system (25:74:1 adjusted to 50:49:1) afforded a white foam in 99% isolated yield. R_f (EtOAc:Tol, 4:1) 0.77, 0.65. FAB-MS (NBA) 833.3; Calcd 833.05.

The dimethoxytrityl-butanediol-*O*-*N*,*N*-diisopropylamino-*O*-(2-cyanoethyl)-phosphoramidite precursor **4a** was purchased from ChemGenes Corp. (Ashland, MA) and was used as received. DNA or 2′F-ANA oligomers containing **3** or **4** were prepared as described

(7) (a) Damha, M. J.; Wilds, C. J.; Noronha, A.; Brukner, I.; Borkow, G.; Arion, D.; Parniak, M. A. *J. Am. Chem. Soc*. **1998**, *120*, 12976−12977. (b) Wilds, C. J.; Damha, M. J. *Nucleic Acids Res*. **2000**, *28*, 3625−3635. (c) Noronha, A. M.; Wilds, C. J.; Lok, C.-N.; Viazovkina, K.; Arion, D.; Parniak, M. A.; Damha, M. J. *Biochemistry* **2000**, *39*, 7050−7062. (d) Damha, M. J.; Noronha, A. M.; Wilds, C. J.; Trempe, J.-F.; Denisov, A.; Gehring, K. *Nucleosides Nucleotides Nucleic Acids* **2001**, *20*, 429−440. (e) Lok, C.-N.; Viazovkina, E.; Min, K.-L.; Nagy, E.; Wilds, C. J.; Damha, M. J.; Parniak, M. A. *Biochemistry* **2002**, *41*, 3457−3467. (f) Elzagheid, M. I.; Viazovkina, E.; Damha, M. J. In *Current Protocols in Nucleic Acid Chemistry*, Unit 1.7; Beaucage, S. L., Bergstrom, D. E., Gli, G. D., Eds.; 2002. (g) Viazovkina, E.; Mangos, M. M.; Elzagheid, M. I.; Damha, M. J. In *Current Protocols in Nucleic Acid Chemistry*, Unit 4.15; Beaucage, S. L., Bergstrom, D. E., Gli, G. D., Eds.; 2002.

(8) (a) Berger, I.; Tereshko, V.; Ikeda, H.; Marquez, V. E.; Egli, M. *Nucleic Acids Res*. **1998**, *26*, 2473−2480. (b) Ikeda, H.; Fernandez, R.; Wilk, A.; Barchi, J. J.; Huang, X.; Marquez, V. E. *Nucleic Acids Res*. **1998**, *26*, 2237−2244. (c) Venkateswarlu, D.; Ferguson, D. M. *J. Am. Chem. Soc*. **1999**, *121*, 5609−5610.

(9) (a) Denisov, A. Y.; Noronha, A. M.; Wilds, C. J.; Trempe, J.-F.; Pon, R. T.; Gehring, K.; Damha, M. J. *Nucleic Acids Res.* **2001**, *29*, 4284−4293. (b) Trempe, J. F.; Wilds, C. J.; Denisov, A. Y.; Pon, R. T.; Damha, M. J.; Gehring, K. *J. Am. Chem. Soc*. **2001**, 123, 4896−4903.

(10) Minasov, G.; Teplova, M.; Wengel, J.; Egli, M. *Biochemistry* **2000**, *39*, 3525−3532.

(11) (a) Mikhailov, S. N.; Pfleiderer, W. *Tetrahedron Lett*. **1985**, *26*, 2059−2062. (b) Nielsen, P.; Dreiøe, L. H.; Wengel, J. *Bioorg. Med. Chem*. **1995**, *3*, 19−28.

(12) Wu, T.; Ogilvie, K. K.; Pon, R. T. *Nucleic Acids Res.* **1989**, *17*, 3501−3517.

Scheme 1 [a]

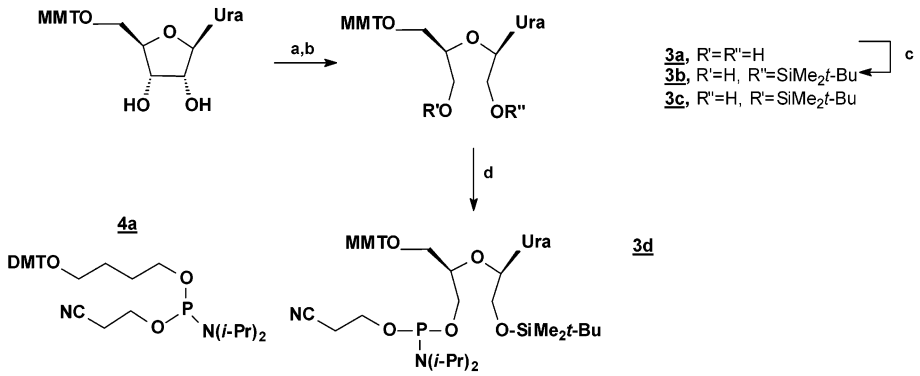

[a] Reactants: (a) $NaIO_4$, dioxane, H_2O, 2 h (quantitative); (b) $NaBH_4$, dioxane, H_2O, 15 min (quantitative); (c) *t*-BDMS-Cl, $AgNO_3$, THF, 24 h (**3b**, 22%; **3c**, 14%); (d) Cl-P(OCE)N(*i*-Pr)$_2$, DMAP, EtN(*i*-Pr)$_2$, THF, 2.5 h (99%).

Table 1. Melting Temperatures (T_m) and RNase H-Mediated Hydrolysis Profiles for the AON/RNA Heteroduplexes[a]

entry	sequence type[b,c] (5′→3′)	T_m (°C)	relative rates (k_{rel}) of enzyme cleavage[d]
	(i) DNA		
I	ttt ttt ttt ttt ttt ttt	39	1
II	ttt ttt ttt Btt ttt ttt	33	2.7
III	tta tat ttt ttc ttt ccc	53	1
IV	tta tat ttt Btc ttt ccc	48	3.4
V	tta tat ttt *c*tc ttt ccc	40	0.7
VI	tta tat ttt B ttc ttt ccc	48	2.5
	(ii) 2′F-ANA		
VII	TTT TTT TTT TTT TTT TTT	53	1
VIII	TTT TBT TTT TTT TTT TTT	49	0.6
IX	TTT TTT TTT BTT TTT TTT	47	7.9
X	TTT TTT TTT TTT BTT TTT	49	5.1
XI	TTT TTT TTT STT TTT TTT	47	1.6
XII	TTT TTT TTS STT TTT TTT	42	2.8
XIII	TTA TAT TTT TTC TTT CCC	64	1
XIV	TTA TAT TTT BTC TTT CCC	55	3.5
XV	TTA TAT TTT CTC TTT CCC	55.5	0.9
XVI	TTA TAT TTT tTC TTT CCC	63	1.6
XVII	TTA TAT TTT B TTC TTT CCC	57	2.3
	(iii) Ha-*ras* AON[e]		
XVIII	att ccg tca tcg ctc ctc	70	33.8
XIX	att ccg tca Bcg ctc ctc	58	31.6
XX	att ccg tca *c*cg ctc ctc	63	31.9
XXI	ATT CCG TCA TCG CTC CTC	82	1
XXII	ATT CCG TCA BCG CTC CTC	72	23.3

[a] Aqueous solutions of 2.38×10^{-6} M of each oligonucleotide, 140 mM KCl, 1 mM $MgCl_2$, 5 mM Na_2HPO_4 buffer (pH 7.2); uncertainty in T_m is ±0.5 °C. [b] Target RNA sequences correspond to rA_{18}, or 5′-r(GGGAAAGAAAAAAUAUAA)-3′. [c] Upper case letters, 2′F-ANA nucleotides; lower case letters, deoxynucleotides; *C*, arabinofluorocytidine or *c*, deoxycytidine mismatch residue; B, butanediol linker; S, 2′-secouridine insert. [d] Human enzyme; rates shown have been obtained at 22 °C and are normalized according to the parent strand of each series except within Ha-*ras* sequences in which data have been obtained at 37 °C and are normalized to all-2′F-ANA AON (entry XXI). [e] Target RNA (40mer) sequence: 5′-r(CGCAGGCCCCUGAGGAGCGAUGACG-GAAUAUAAGCUGGUG)-3′; underlined residues denote the region in the RNA to which the AON binds.

previously,[7a,b] and were characterized by analytical PAGE, anion exchange HPLC, and MALDI-TOF mass spectrometry. Sequences of the oligonucleotides used are provided in Table 1.

UV Thermal Denaturation Measurements. AON and complementary target RNA oligonucleotides were mixed in equimolar ratios in 140 mM KCl, 1 mM $MgCl_2$, and 5 mM Na_2HPO_4 buffer, pH 7.2, to provide a total duplex concentration of ca. 5 μM. Samples were heated to 90 °C for 15 min and then cooled slowly to room temperature, and stored at 4 °C overnight before measurements. The AON/RNA duplex solution was then exposed to increasing temperature at 1-min intervals (0.5 °C/measurement), and the UV absorbance at 260 nm was determined after temperature equilibration. T_m values were calculated using the baseline method and have an uncertainty of ±0.5 °C.

Purification of RNase H. *Escherichia coli* RNase HI was purified as described previously.[13] Human RNase HII was overexpressed and purified according to the method of Wu et al.[14]

RNase H Assays. RNase H assays were carried out at 14−15 °C or room temperature (ca. 22 °C), with the exception of Ha-*ras* derived sequences in which assays were conducted at 37 °C. Nucleic acid duplex substrates were prepared by mixing the AON (3 pmol) with 5′-^{32}P-labeled complementary target RNA (1 pmol) in 10 μL of 60 mM Tris-HCl (pH 7.8) containing 60 mM KCl and 2.5 mM $MgCl_2$, followed by heating at 90 °C for 2 min and slow cooling to room temperature. Duplex substrate solutions were allowed to stand at room temperature for at least 1 h prior to use. Reactions were initiated by the addition of human RNase HII or *E. coli* RNase HI, and aliquots were removed at various times and quenched by the addition of an equal volume of 98% deionized formamide containing 10 mM EDTA, 1 mg/mL

(13) Yang, W.; Hendrickson, W. A.; Kalman, E. T.; Crouch, R. J. *J. Biol. Chem.* **1990**, *265*, 13553−13559.
(14) Wu, H.; Lima, W. F.; Crooke, S. T. *J. Biol. Chem.* **1999**, *274*, 28270−28278.

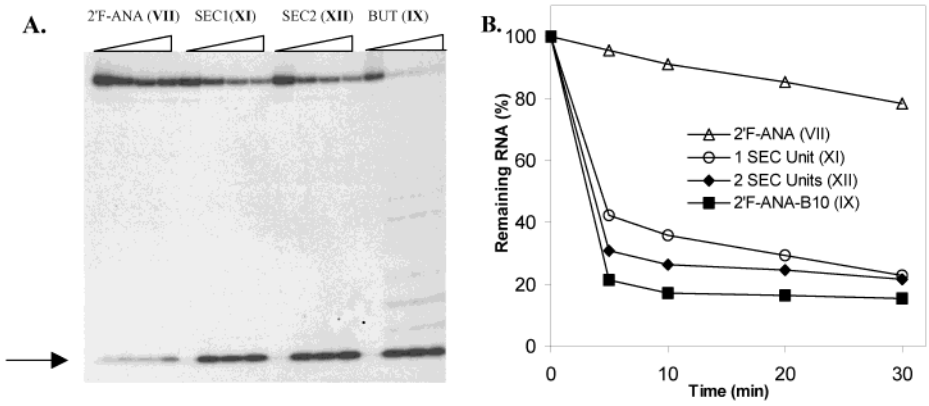

Figure 2. (A) PAGE results showing RNase H-mediated cleavage of duplexes. Assays comprised 1 pmol of target 5′-[^{32}P]-rA_{18} and 3 pmol of test AON in buffer (10 μL) consisting of 60 mM Tris-HCl (pH 7.8), 2 mM dithiothreitol, 60 mM KCl, and 2.5 mM $MgCl_2$. Reactions were started by the addition of human RNase HII (22 °C; lanes: 0, 5, 10, 20, 30 min); arrow indicates coalesced 5′-scission products obtained from multiple cleavage within the same target strand. (B) Quantification of remaining full-length [^{32}P]-RNA obtained by UN-SCAN-IT software (Silk Scientific; Orem, UT).

bromophenol blue and 1 mg/mL xylene cyanol. After heating at 100 °C for 5 min, reaction products were resolved by electrophoresis on 16% polyacrylamide sequencing gels containing 7 M urea, visualized by autoradiography, and product formation was quantified by densitometry.

Results and Discussion

Duplexation Studies. In assessing the thermal behavior of the AONs, we have noted without exception that a drop in stability is characteristic of all strands with single acyclic inserts (Table 1). While this was expected for butyl-containing AONs, we were somewhat surprised that **3** offered no improvement in binding affinity relative to the former. The effect was approximately additive upon incorporating a second secouridine residue, suggesting minimal base pairing or interresidue base stacking. The extent to which the linkers were destabilizing was also contingent upon base sequence, that is, mixed 2′-fluoro-arabino sequences with the butanediol linker **4** were ca. 3 °C more destabilizing than their homopolymeric counterparts (**IX** and **XIV**). Single substitutions were also less tolerated at the center (**IX**; $\Delta T_m = -6$ °C) as opposed to the ends of the sequences (**VIII** and **X**; $\Delta T_m = -4$ °C), which is an expected and recurrent phenomenon[11b,15] that is manifest from end-fraying of the duplex.

Interestingly, placement of a C−A mismatch in either of the mixed-sequence AON backbones significantly destabilizes their hybrids with RNA, with the deoxy sequences proving less competent toward retaining adequate target avidity as compared to the 2′F-ANA complements. Furthermore, only modest destabilization occurs upon insertion of one deoxynucleotide in the all-2′F-ANA mixed sequences, which is consistent with the notion that the arabinofluoro residues enhance thermal stability via strand preorganization over the native residues yet do not perturb the stereoregular structure of the AON to any appreciable degree.[7a,8,9]

RNase H Assays. Fortunately, the destabilization introduced into the AON by the acyclic linkers is largely outweighed by the high stabilization[7,9] afforded by the rigid 2′F-ANA backbone. Indeed, when linked to a proven RNase H-competent analogue, for example, 2′F-ANA,[7−9] an acyclic insert in the middle of an 18-nt oligomer enhances RNase H-assisted sense strand hydrolysis (Figure 2). Moreover, a second contiguous insert amplifies the effect, whereas the incorporation of a single butanediol insert in the middle of the same sequence potentiates the targeted destruction of the AON-chimera:substrate duplex even further, as much as ca. 8-fold relative to the uniformly modified control AON (Table 1, e.g., **VII** and **IX**). This methodology is entirely applicable in DNA backbones as well, in which the relative rate enhancements easily approach a 3-fold improvement in target degradation over the native strands (e.g., **I** vs **II**; **III** vs **IV**). The enhancement in rate, coupled with a distinct cleavage pattern upstream of the site of the inserts in the AON, is also apparent in mixed-sequence analogues (see Supporting Information), suggesting the generality of the structural effects on the conformational discretion of the human enzyme.

A possible, yet partial, explanation for the elevated RNA degradation may owe to an increased turnover efficiency of the enzyme for the linker-modified duplexes, which may arise from an enhanced rate of dissociation for these hybrids over their thermostable counterparts (e.g., $\Delta T_m = -9$ °C for **XIV** vs **XIII**). For instance, 2′F-ANA, which forms stronger duplexes, exhibits reduced turnover relative to DNA and 2′F-ANA-B10 hybrids, and therefore would seem to accommodate such a trend (see Supporting Information). On the other hand, the activity is diminished in mismatched DNA and 2′F-ANA AON mixed sequences, where a respective deoxy- or arabinofluorocytidine mismatch replaces the butyl linker (Table 1, **V** and **XV**). Because the mismatch also induces an equivalent (2′F-ANA) or larger (DNA) drop in duplex thermal stability relative to the butyl insertion, it appears that increased turnover is not the sole basis for preferential enzyme discrimination toward the flexible AONs in these examples. We further speculate that residual activity is retained in mismatched sequences by virtue of this characteristic *alone* (i.e., increased turnover), which now becomes operative in segments of partial complementarity.

Linker Position. To examine the relevance of enzyme turnover efficiency and of the actual cleavage event in other contexts, we next prepared AONs with linker **4** at various positions to determine whether optimal activity is dependent upon the site of the insertion. Moreover, this strategy should lend further credibility to the precise pattern and rate of cleavage

(15) Vandendriessche, F.; Augustyns, K.; Aerschot, A. V.; Busson, R.; Hoogmartens, J.; Herdewijn, P. *Tetrahedron* **1993**, *49*, 7223−7238.

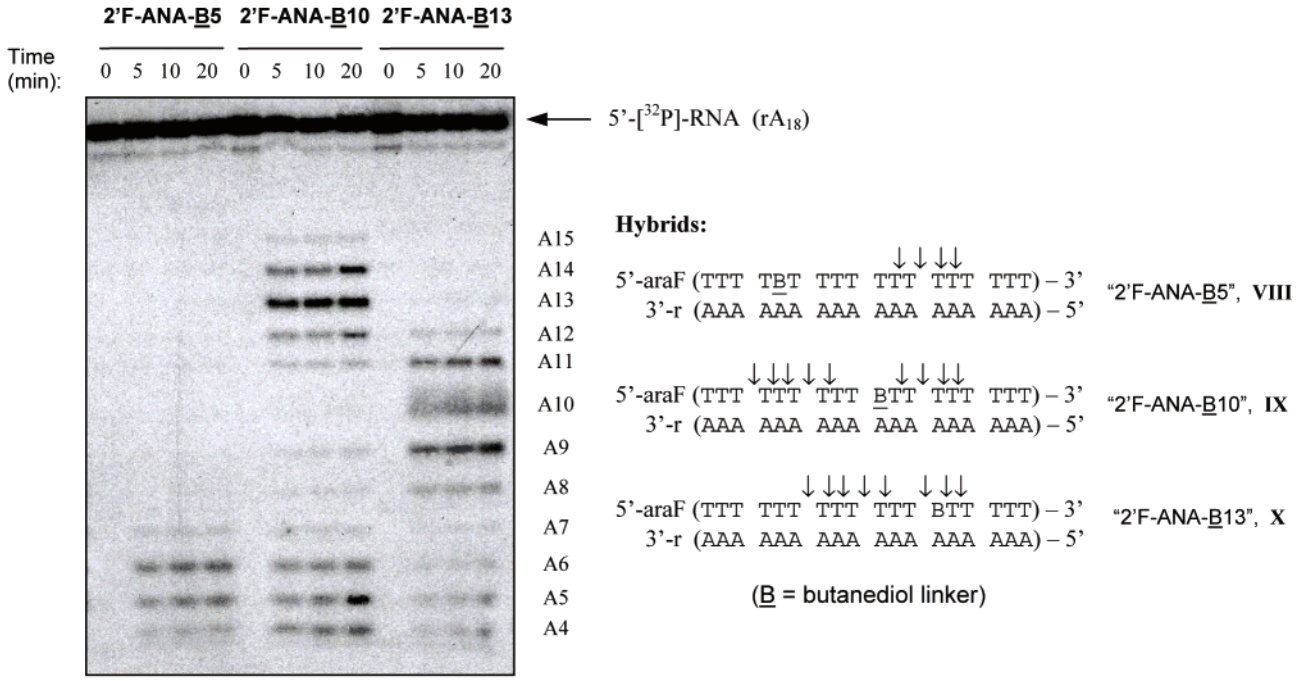

Figure 3. Gel (PAGE) showing linker-dependent human RNase HII-mediated hydrolysis patterns of duplexes. Assays (10 μL final volume) comprised 1 pmol of 5′-[^{32}P]-target RNA and 3 pmol of test oligonucleotide in 60 mM Tris-HCl (pH 7.8, containing 2 mM dithiothreitol, 60 mM KCl, and 10 mM $MgCl_2$. Reactions were started by the addition of RNase H and carried out at 14−15 °C for 20 min. Lengths of the RNA fragments generated via enzyme scission and corresponding position along the AON are indicated.

that accompanies the movement of the linker along the 2′F-ANA backbone (Table 1 and Supporting Information).

Close inspection of the autoradiogram in Figure 2 reveals that the exact location of RNase H-executed primary cuts on the RNA strand is difficult to measure under ambient temperature for the homopolymers, which are already known to be good substrates for the enzyme. As we were now interested to see where the first cuts were occurring, this information was instead extracted from assays conducted at the lower temperature, under which enzyme activity is retarded just enough to enable a qualitative comparison on the preferred cleavage modes toward each substrate (Figure 3). At higher temperatures, the pattern becomes less interpretable as it results from the superimposition of multiple cleavages on a single target by the enzyme (Figure 2).

We observe an overall enhancement in target degradation in the order of 2′F-ANA-B10 (**IX**) > 2′F-ANA-B13 (**X**) > 2′F-ANA (**VII**) > 2′F-ANA-B5 (**VIII**). Furthermore, all of the butyl-containing AONs induce additional primary cuts at the 3′-end of the RNA except for 2′F-ANA-B5, which coincidentally, is the only AON superseded in rate by all-2′F-ANA. As such, the B5 and B13 homopolymeric substrates show large differences in activation potencies, although their sequences are virtually identical and equally thermostable, yet with opposite directionalities with respect to the butyl site in the AON. Indeed, the different activities of these two compositions contrast their thermal and structural similarities, and suggest a minor—if not absent—role for the turnover effect. The diminished rate enhancement in the AON with butyl at position 5 might alternatively reflect the remote positioning of RNase H along the substrate, which is known to bind near the 3′-end of the AON in the hybrid duplex[13] and so may be unaffected by the butyl insertion. This does not explain, however, why there is a reduction relative to 2′F-ANA, although an adverse effect on the catalytic activity of the enzyme—which initiates cleavage upstream with respect to the binding along the hybrid—may be accountable.

Table 2. Relative Rates of RNA Target[a] Degradation among Mixed-Sequence DNA and 2′F-ANA AON Constructs

entry	sequence type[b]	k_{rel} (human)[c]	k_{rel} (*E. coli*)[c]
III	DNA	4.6	8.8
V	DNA-*c*10	3.3	7.1
XIII	2′F-ANA	1.0	1.0
XIV	2′F-ANA-B10	3.5	1.4
XV	2′F-ANA-*C*10	0.9	1.3
XVI	2′F-ANA-t10	1.6	2.6

[a] Target RNA: 5′-r(GGG AAA GAA AAA AUA UAA)-3′. [b] AON sequences are abbreviated as follows: *c*10, *C*10 B10 and t10 denote deoxycytidine, arabinofluorocytidine, butyl, or deoxythymidine residue in place of the 10th nucleotide in the AON, respectively; complete description is given in Table 1. [c] Assays were conducted at 22 °C; rates are normalized according to the all-2′F-ANA AON (**XIII**).

2′F-ANA vs DNA in Human and *E. coli* Isotypes. These findings prompted us to explore the activating potential of our purely artificial 2′F-ANA constructs *directly* to those of oligonucleotides mainly containing deoxyribose residues in the antisense strand. While a mismatching residue in either 2′F-ANA or DNA mixed-base sequences imposes a negligible effect on the overall enzyme hydrolytic efficiency as compared to the parent AONs, a substantial acceleration in degradation rate is readily achieved by sequences incorporating a modest degree of flexibility in the antisense strand (Table 2). For example, substitution of a central arabinofluoro residue in 2′F-ANA **XIII** with a more flexible deoxy sugar (**XVI**) elevates the activity of both RNase H isotypes. In the human system, an immediate and pronounced increase in target degradation is likewise apparent upon interchange of a deoxythymidine in the rigid 2′F-ANA antisense for a butyl linker (AON **XIV**), which closes

the efficiency gap between 2′F-ANA (k_{rel} 3.5) and DNA-derived (k_{rel} 4.6) AON considerably.

Even more intriguing is the finding that the preference for a more flexible duplex substrate is a property displayed by the bacterial (*E. coli*) enzyme as well, such that target strand hydrolysis is accelerated in the presence of a single deoxy or butyl insert within the parent AON (Table 2). It is noteworthy, however, that the discriminatory properties of the two isotypes display some subtle variations. Specifically, the bacterial homologue shows greater tolerance for deoxythymidine-containing constructs over the butyl-containing 2′F-ANA strands, in contrast to that observed with its human counterpart. The reasons for this disparity are presently unclear but could be related to variations in the placement of catalytically active residues between the two isotypes. These may ultimately result in subtle differences in the way these homologues interact with a particular substrate type. Unfortunately, the lack of definitive structural data regarding the physical dimensions of the class II enzyme's binding and catalytic cavities render this hypothesis merely presumptive at present.

Effect of "Looping" Butyl Linker. As enzyme efficiency may be related to the energetic cost of distorting the duplex into a more catalytically reactive conformation, placing the linker outside of the helix should enable closer scrutiny into the dynamic nature of the RNase H−AON complex interaction. As such, when the nonnucleotidic linker is shifted *outside* of the helix by inserting a nucleotide complementary to the RNA single-gap region (e.g., **VI** and **XVII**, Table 1), this gives an oligonucleotide of 19 units in length with two nonameric nucleotide segments that are capable of forming perfect complexes with the RNA.

In this regard, the 2′F-ANA-B-Lp sequence (**XVII**, Table 1) contains unifying elements of both the 2′F-ANA (**XIII**) and 2′F-ANA-B10 (**XIV**) mixed-sequence oligonucleotides. These consist of a localized flexible site in the center of the sequence (similar to 2′F-ANA-B10) as well as the ability to fully hybridize with the target RNA (similar to 2′F-ANA). For this sequence, AON binding to the RNA is likely accompanied by a local compression of the AON backbone at the extrahelical site to project or "loop" the linker away from the duplex core. Such a compensatory distortion of the helix may further be reconciled through kinking in the overall conformation of the hybrid which probably also occurs to maximize the number of residues that form base pairs between this oligonucleotide and the RNA. This is reflected in a modest gain in the thermal stability of this sequence relative to that of 2′F-ANA-B10 ($\Delta T_m = 2$ °C), which although not as high as that of all-2′F-ANA, indicates that some linker-induced motility of the strands surrounding the junction may be necessary to relieve local intrastrand steric effects.

In contrast, DNA with a looping butyl linker (DNA-B-Lp, **VI**) is incapable of promoting stable base pairing between butyl-anchoring residues and the opposing RNA strand, as this sequence exhibits the same thermal stability as when the linker resides completely parallel with the helix axis (e.g., AON **IV**). This is not entirely unexpected however, as the deoxynucleotides themselves are considerably more flexible than 2′F-ANA residues and so would be more likely to experience greater intrahelical disorder around the backbone region flanking the linker insertion.

In either case, we speculated that forcing the linker out of the helix in this manner could potentially disrupt some of the interactions between RNase H and the two strands by reducing the number of stable contacts between the enzyme and the duplex minor groove. Remarkably, enzyme assays with both 2′F-ANA-B-Lp and the analogous DNA-derived oligonucleotides suggest that such a protrusion is only associated with a minor energy penalty for enzyme docking and subsequent processive activities. In fact, both the DNA and 2′F-ANA sequences still considerably enhance RNA degradation (compare oligomers **XIII** vs **XVII** and **III** vs **VI**, Table 1), which suggests that flexibility in the antisense strand is important for effective RNase H induction, *irrespective of whether the flexible linker resides directly within or extends away from the helix axis*.

The converse is true when a mismatching residue occupies a central position within the antisense strand. For instance, the mismatched nucleotide in DNA-*c*10 (**V**) and 2′F-ANA-*C*10 (**XV**) oligonucleotides should likewise occupy an external position along the hybrid duplex (similar to "B-Lp" AONs **VI** and **XVII**), as steric prohibition with the opposing RNA nucleotide likely occurs to "bulge" the mismatch away from the helix. However, if proper enzyme interaction with these substrates necessitates subtle repositioning of the strands within the AON:RNA complex, a high energy penalty associated with this event could reduce the enzyme's overall capacity to bind to and cleave the mismatched substrates. This presumably disables extensive processing in these duplexes as opposed to an inherently flexible alternative. In the butyl-modified duplexes where the linker loops out of the helix, enzyme activation is conceivably retained as steric interactions are relieved via an induced spatial rearrangement of the linker by the enzyme upon substrate docking. It is especially noteworthy that a possible transient delay in catalysis due to such repositioning of the looping linker during the enzyme interaction may be responsible for the reduced rates relative to DNA- (**IV**) and 2′F-ANA-B10 (**XIV**) substrates in which the linker resides parallel with the helix and likely requires minimal distortion.

Ha-*ras* RNA. As the extent and rate of RNA cleavage should also depend on the structure, length, and base composition of the target polyribonucleotide, we next evaluated whether the flexible AONs could accelerate cleavage in a highly structured, physiologically relevant RNA species.

We particularly examined the specific reduction of target RNA levels using an in vitro Ha-*ras* model system, especially since hyperactivated forms of both point mutant and nonmutated mammalian c-*ras* protooncogenes are frequently implicated in various human cancers,[16] thus making this a desirable therapeutic target. As such, the linker-modified antisense oligonucleotides were directed to hybridize with an internal 18-nucleotide region in the c-*ras* mRNA encompassing the translation initiation site of the *ras* gene and corresponding to residues −19 to +21 of the full length transcript.

Possible secondary structures of the c-*ras* target RNA were extracted using the MFOLD program[17] which estimates ΔG°_{37} values for self-complementary duplex formation (available at

(16) (a) Chakraborty, A. K.; Cichutek, K.; Duesberg, P. H. *Proc. Natl. Acad. Sci. U.S.A.* **1991**, *88*, 2217−2221. (b) Hua, V. Y.; Wang, W. K.; Duesberg, P. H. *Proc. Natl. Acad. Sci. U.S.A.* **1997**, *94*, 9614−9619.

(17) (a) Zuker, M.; Mathews, D. H.; Turner, D. H. In *RNA Biochemistry and Biotechnology* 11−43; Barciszewski, J., Clark, B. F. C., Eds.; Kluwer Academic Publishers: Norwell, MA, 1999. (b) Mathews, D. H.; Sabina, J.; Zuker, M.; Turner, D. H. *J. Mol. Biol.* **1999**, *288*, 911−940.

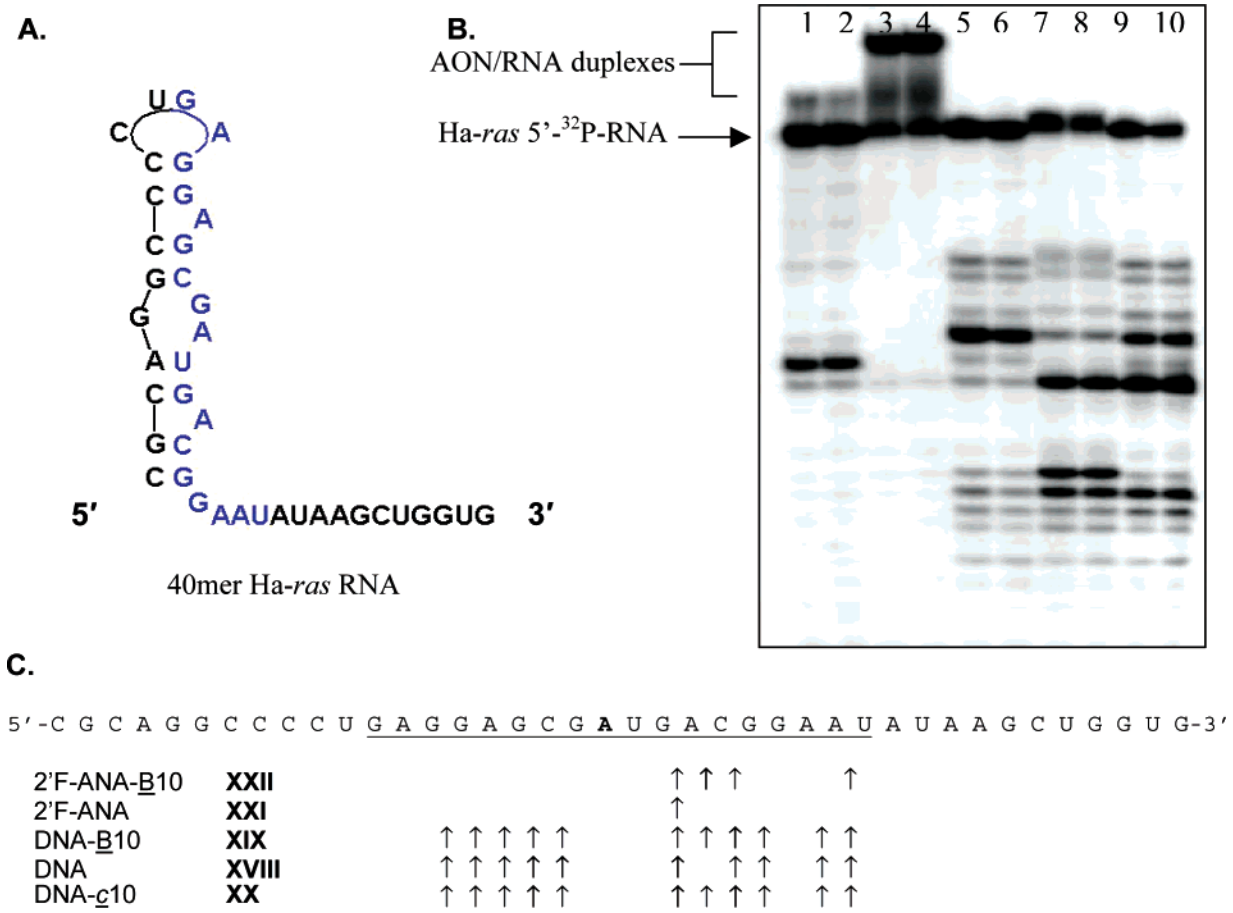

Figure 4. (A) Probable secondary structure adopted by 40mer Ha-*ras* RNA, predicted using the Turner−Zuker algorithm.[17] Residues in blue denote the region to which the AON binds. (B) Denaturing PAGE illustrating human RNase HII-mediated cleavage of 5′-^{32}P-labeled Ha-*ras* RNA (1 pmol) duplexed with mixed base AON sequences (5 pmol) at 37 °C. Lanes 1 and 2: 2′F-ANA-B10-**XXII**, 10 and 20 min; lanes 3 and 4: 2′F-ANA-**XXI**, 10 and 20 min; lanes 5 and 6: DNA-B10-**XIX**, 10 and 20 min; lanes 7 and 8: DNA-**XVIII**, 10 and 20 min; lanes 9 and 10: DNA-*c*-10-**XX**, 10 and 20 min. The slowly migrating band in lanes 3 and 4 is the 2′F-ANA:RNA duplex (T_m > 80 °C) which withstands the denaturing conditions of the gel electrophoresis and the heating of the sample prior to being loaded onto the gel; see Table 1 for complete list of sequences. (C) Lengths of the RNA fragments generated via enzyme scission and corresponding position along the AON. Bold arrows represent the major cleavage sites; the highlighted A residue in the RNA sequence denotes the residue opposite the insertion position of the linker in the AON. Kinetic data (k_{rel}) of RNA cleavage is provided in Table 1.

http://bioinfo.math.rpi.edu/~zukerm/rna/). Although the program employed is based on parameters generated from the folding of RNA under high ionic solution conditions (i.e., 1 M NaCl), these calculations argue for the existence of a single predominant species in which most of the target site (ca. 75%) is sequestered in a stable 25-base hairpin structure (Figure 4A). This prediction is supported by analysis of the UV thermal profile of the 40mer, which indicates biphasic melting behavior likely due to structural changes induced by the unfolding of the RNA or denaturation of self-associated (i.e., intermolecular) RNA complexes. That all of these characteristics are closely reproduced in a longer *ras*-derived target spanning residues −24 to +26 of the full length transcript, further corroborates these observations (data not shown).

For DNA-based AONs within this series, an increase in human RNase HII-mediated target degradation is not apparent upon interchanging a deoxynucleotide residue in the parent strand for a butanediol linker (i.e., **XVIII** and **XIX**; Table 1 and Figure 4) and appears to be consistent with prior work by other groups.[18]

Alternatively, this effect may be explained in part by a decreased propensity for this AON to associate with the RNA, resulting in a nonhomogeneous AON:RNA population and consequently a lesser amount of substrate duplex presented to the enzyme for cleavage. Duplex heterogeneity seems even more likely given that hybrid formation with DNA-B10-**XIX** produces the least intrinsically stable duplex within the series (Table 1). Consequently, greater competition for intramolecular folding of the target as opposed to intermolecular duplexation could conceivably mask any observable differences in cleavage rates.

However, this is not the case for the 2′F-ANA constructs. As demonstrated throughout this work, substitution of the arabinofluoronucleoside residue in 2′F-ANA with a more flexible butanediol linker elevates the activity of RNase HII considerably, ca. 23-fold over the parent compounds and approaching the level of enzyme-induced degradation attainable with the native oligodeoxynucleotides. Once again, these properties are consistently reproduced when the 2′F-ANA-based constructs are directed against a slightly longer c-*ras* 50mer RNA (data not shown), indicating that a significant enhancement

(18) (a) Vorobjev, P. E.; Pyshnaya, I. A.; Pyshnyi, D. V.; Repkova, M. N.; Venyaminova, A. G.; Zenkova, M. A.; Ivanova, E. M.; Scalfi-Happ, C.; Seliger, H.; Bonora, G.; Zarytova, V. F. *Bioorg. Khim.* **2000**, *26*, 844−851. (b) Vorobjev, P. E.; Pyshnaya, I. A.; Pyshnyi, D. V.; Venyaminova, A. G.; Ivanova, E. M.; Zarytova, V. F.; Bonora, G.; Seliger, H. *Antisense Nucleic Acid Drug Dev.* **2001**, *11*, 77−85.
(19) Toulmé, J.-J.; Frank, P.; Crouch, R. J. In *Ribonucleases H*; Crouch, R., Toulmé, J.-J., Eds.; INSERM: Paris, France 1998; p 147.

in target hydrolysis may readily be achieved by the butyl-modified AON, even when targeting a highly structured RNA species.

Conclusions

As such, a balance between flexibility and rigidity in the AON appears to be essential for enhancing targeted destruction of the hybrid duplex by RNase H, provided that the geometrical elements around the actual cleavage site still retain the necessary requirements that have thus far been demonstrated—that is, Eastern sugar conformation and B-form[7d,8c,9] character in the AON strand. Indeed, 2′F-ANA-B constructs (e.g., **XIV**) represent the first examples of modified AON devoid of deoxyribose sugars that elicit RNase H activity with comparable efficiency to the native (DNA) systems. We speculate that the malleability of the duplex backbone region surrounding the acyclic modifications likely better accommodates the enzyme into the minor groove[4a,b,19] and may aid in more efficient hydrolysis during the catalytic event, thereby giving rise to the observed rate enhancements.

We are presently undertaking further studies with these and other acyclic analogues as well as extending our knowledge to other RNase H isozymes. These endeavors should afford valuable insight into the substrate requirements of the enzyme and provide a versatile method in generating a new repertoire of more potent antisense compounds.

Acknowledgment. This work is dedicated to Professor Kelvin K. Ogilvie on the occasion of his 60th birthday. We thank R. T. Pon and S. Carriero for synthesis and purification of the 40mer Ha-*ras* RNA, respectively. M.J.D. and M.A.P. gratefully acknowledge support from CIHR (Canada) and Anagenis, Inc.

Supporting Information Available: A table of calculated extinction coefficients and mass spectral data (MALDI-TOF); gels of DNA-B10 oligothymidylates, mixed-sequence 2′F-ANA-B10; and relative turnovers of 2′F-ANA, dT_{18}, and 2′F-ANA-B10 oligothymidylates (PDF). This material is available free of charge via the Internet at http://pubs.acs.org.

JA025557O